AIAA JOURNAL
Vol. 35, No. 1, January 1997

Finite Element Method for Nonlinear Free Vibrations of Composite Plates

Yucheng Shi,* Raymond Y. Y. Lee,* and Chuh Mei†
Old Dominion University, Norfolk, Virginia 23529-0247

A multimode time-domain modal formulation based on the finite element method for large-amplitude free vibration of thin composite plates is presented. Accurate frequency–maximum deflection relations can be predicted for the fundamental and the higher nonlinear modes. A modal participation is defined, and accurate and convergent frequencies can be determined with minimum number of linear modes. A procedure for the selection of initial conditions for periodic plate response is presented. Convergence of frequency with gridwork refinement and number of linear modes is studied. The classical single-mode elliptic function frequency solutions for simply supported beams and square plates are assessed. Examples of orthotropic and composite plates are given, and the characteristics of nonlinear response are studied.

Introduction

THE subject of large-amplitude vibrations of beams and plates has been of constant interest to many investigators since the first revelation of the classical analytical elliptic function solutions of simply supported beams by Woinowsky-Krieger[1] and rectangular plates by Chu and Herrmann.[2] Whitney and Leissa[3] have formulated the governing equations for large-amplitude vibrations of heterogeneous anisotropic plates in the von Kármán sense. Based on these equations, various approximate solution procedures and results have been reported by numerous investigators. An excellent review of classic continuum approaches for geometrically nonlinear analysis of composite plates was given by Chia.[4] Chia has also considered the nonlinear response of various types of plates in his excellent monograph.[5] Sathyamoorthy[6] has presented a comprehensive survey of nonlinear vibration analysis of plates using approximate analytical and finite element methods.

Srirangaraja[7] recently presented two alternative solutions for the large-amplitude free vibration of a simply supported beam. The two approximate solutions are based on the method of multiple scales (MMS) and the ultraspherical polynomial approximation (UPA) method. The frequency ratios for the fundamental mode, $(\omega/\omega_L)_1$, at the ratio of beam maximum deflection to radius of gyration of 5.0 ($w_{\max}/r = 5.0$) are 3.3438 and 3.0914 using the MMS and UPA methods, respectively. The frequency ratios from nine other different methods, a total of 11, in the literature were also given in Table 1 of Ref. 7. It is rather surprising that the frequency ratio for the fundamental mode at $w_{\max}/r = 5.0$ for a simply supported beam varied in such a wide range[7]: from the lowest of 2.0310 (harmonic oscillations assumption) to the highest of 3.3438 (MMS) and with the elliptic function solution at 2.3501 by Woinowsky-Krieger.[1] The other methods and the frequency ratios at $w_{\max}/r = 5.0$ are energy balance (2.3848), Galerkin and perturbation (2.3848), finite element (2.3502), and harmonic balance (2.3489).

Similarly, large variations existed for the vibration of plates. Rao et al.[8] presented a finite element approach for the large-amplitude free flexural vibration of plates. The fundamental frequency ratios for a simply supported square plate from six different methods were reported (see Table 1 of Ref. 8). The frequency ratio at $w_{\max}/h = 1.0$ varied from a low of 1.2967 to the high of 1.5314 with Chu and Herrmann's[2] analytical solution at 1.4023. The questions are then the following: 1) Are the single-mode fundamental frequency results by Woinowsky-Krieger[1] and Chu and Herrmann[2] accurate, and 2) how can accurate frequencies for fundamental and higher nonlinear modes for composite plates be obtained?

This paper presents a time-domain modal formulation using the finite element method for large-amplitude free vibrations of generally laminated thin composite rectangular plates. Selection of the proper initial conditions for periodic plate motions is presented. Accurate frequency ratios for fundamental as well as higher modes of composite plates at various maximum deflections can be determined. Isotropic beam and plate can be treated as special cases of the composite plate. Percentage of participation from each linear mode to the total plate deflection can be obtained, and thus an accurate frequency ratio using a minimum number of linear modes can be assured. Another advantage of the present finite element method is that the procedure for obtaining the modal equations of the general Duffing-type is simple when compared with the classical continuum Galerkin's approach.

Formulation

The finite element system equations of motion for the large-amplitude free vibration of a thin laminated composite plate can be expressed as[9]

$$\begin{bmatrix} [M]_b & 0 \\ 0 & [M]_m \end{bmatrix} \begin{Bmatrix} \ddot{W}_b \\ \ddot{W}_m \end{Bmatrix} + \left(\begin{bmatrix} [K]_b & [K_B] \\ [K_B]^T & [K]_m \end{bmatrix} + \begin{bmatrix} [K1_{Nm}] + [K1_{NB}] & [K1]_{bm} \\ [K1]_{mb} & 0 \end{bmatrix} + \begin{bmatrix} [K2]_b & 0 \\ 0 & 0 \end{bmatrix} \right) \begin{Bmatrix} W_b \\ W_m \end{Bmatrix} = 0 \tag{1a}$$

or

$$[M]\{\ddot{W}\} + ([K] + [K1] + [K2])\{W\} = 0 \tag{1b}$$

where $[M]$ and $[K]$ are constant matrices and represent the system mass and linear stiffness, respectively; $[K1]$ and $[K2]$ are the first-order and second-order nonlinear stiffness matrices, respectively; $[K1_{Nm}]$ depends linearly on the unknown membrane displacements $(\{N_m\} = [A]\{\epsilon_m^0\} = [A][B_m]\{W_m\})$ and represents the bending stiffness induced by the linear membrane strains $\{\epsilon_m^0\}$; $[K1_{NB}]$ depends linearly on the unknown bending displacements $(\{N_B\} = [B]\{\kappa\} = [B][B_b]\{w_b\})$ and represents the bending stiffness induced by the extension-bending laminate coupling $[B]$ and curvatures $\{\kappa\}$; $[K1]_{bm}$ depends linearly on the unknown plate slopes and represents the coupling between membrane and bending

Received April 4, 1996; revision received Sept. 12, 1996; accepted for publication Sept. 13, 1996; also published in *AIAA Journal on Disc*, Volume 2, Number 1. Copyright © 1996 by the American Institute of Aeronautics and Astronautics, Inc. All rights reserved.

*Graduate Student, Department of Aerospace Engineering. Student Member AIAA.

†Professor, Department of Aerospace Engineering. Associate Fellow AIAA.

displacements due to large deflection; and $[K2]_b$ depends quadratically on the unknown plate slopes and represents the bending stiffness induced by the nonlinear membrane strains $\{\epsilon_b^0\}$ due to large deflection. The subscripts b and m denote bending and membrane components, respectively. The element mass, linear stiffness, and nonlinear stiffness matrices are all symmetrical and can be found in Ref. 9. Most of the finite element large-amplitude free vibration results for plates and beams (a special case of plate) in the literature were based on Eq. (1) using certain approximate procedures in conjunction with an iterative scheme (e.g., Refs. 8 and 9 and others).

The system equations of motion presented in Eq. (1) are not suitable for numerical integration because 1) the nonlinear stiffness matrices are functions of the unknown displacements, and (2) the number of degrees of freedom (DOF) of the system nodal displacements $\{W\}(=\{W_b, W_m\}^T)$ is too large. Therefore, Eq. (1) has to be transformed into the modal coordinates of much smaller DOF, and also the Duffing-type modal equations would involve only constant nonlinear modal stiffness matrices. This is accomplished by a modal transformation and truncation

$$\{W\} = \sum^{n} q_r(t)\{\phi\}^{(r)} = [\Phi]\{q\} \tag{2}$$

where the number of retained linear modes n is much smaller than the system nodal DOF. The normal mode $\{\phi\}^{(r)}$ (normalized with the maximum component to unity) and linear frequency ω_{Lr} are obtained from the linear vibration solution of the system

$$\omega_{Lr}^2[M]\{\phi\}^{(r)} = [K]\{\phi\}^{(r)} \tag{3}$$

The nonlinear stiffness matrices $[K1]$ and $[K2]$ in Eq. (1) can be expressed as the sum of the products of modal coordinates and nonlinear modal stiffness matrices

$$[K1] = \sum^{n} q_r[K1]^{(r)} \tag{4}$$

and

$$[K2] = \sum^{n}\sum^{n} q_r q_s[K2]^{(rs)} \tag{5}$$

The nonlinear modal stiffness matrices $[K1]^{(r)}$ and $[K2]^{(rs)}$ are assembled and evaluated with the corresponding element components $\{w_b\}^{(r)}$ and $\{w_m\}^{(r)}$ obtained from the known system linear mode $\{\phi\}^{(r)}$ as

$$[K1]^{(r)} = \sum_{\substack{\text{all elements}\\ +\text{bdy. conds.}}} \begin{bmatrix} [k1_{Nm}]^{(r)} + [k1_{NB}]^{(r)} & [k1]_{bm}^{(r)} \\ [k1]_{mb}^{(r)} & 0 \end{bmatrix} \tag{6}$$

and

$$[K2]^{(rs)} = \sum_{\substack{\text{all elements}\\ +\text{bdy. conds.}}} \begin{bmatrix} [k2]_b^{(rs)} & 0 \\ 0 & 0 \end{bmatrix} \tag{7}$$

where $[k1]^{(r)}$ and $[k2]^{(rs)}$ represent the element nonlinear modal stiffness matrices. Thus, the nonlinear modal stiffness $[K1]^{(r)}$ and $[K2]^{(rs)}$ are constant matrices.

With the modal transformation of Eq. (2) and the constant nonlinear modal stiffness matrices defined in Eqs. (6) and (7), the system equations of motion (1) are thus transformed to the general Duffing-type modal equations in reduced DOF as

$$[\bar{M}]\{\ddot{q}\} + ([\bar{K}] + [K_q] + [K_{qq}])\{q\} = 0 \tag{8}$$

where the diagonal modal mass and linear stiffness matrices are

$$([\bar{M}], [\bar{K}]) = [\Phi]^T([M], [K])[\Phi] \tag{9}$$

and the quadratic and cubic terms in $\{q\}$ are

$$[K_q]\{q\} = [\Phi]^T\left\{\sum^{n} q_r[K1]^{(r)}\right\}[\Phi]\{q\} \tag{10}$$

and

$$[K_{qq}]\{q\} = [\Phi]^T\left\{\sum^{n}\sum^{n} q_r q_s[K2]^{(rs)}\right\}[\Phi]\{q\} \tag{11}$$

All of the modal matrices in Eq. (8) are constant matrices. With given initial conditions, the response of modal amplitudes $\{q\}$ can be determined from Eq. (8) using any numerical integration scheme such as the Runge–Kutta or Newmark-β method. For periodic plate oscillation with a time period T, the response of all modal coordinates should have the same period T, $q_r(t) = q_r(t+T)$, $r = 1, 2, \ldots, n$. Since initial conditions will affect greatly the modal response, the determination of initial conditions for periodic plate oscillation is to relate each of the rest (usually the higher) modal coordinates in odd powers of the dominated (usually the fundamental) coordinate as

$$\begin{aligned} & a_{r-1}q_1(t; IC) + b_{r-1}q_1^3(t; IC) + c_{r-1}q_1^5(t; IC) + \ldots \\ & = q_r(t; IC), \qquad r = 2, 3, \ldots, n \end{aligned} \tag{12}$$

where the a_is, b_is, and c_is, ..., are constants to be determined and IC denotes initial conditions. For a two-mode ($n = 2$) system, it is accurate enough to keep up to the cubic term only in Eq. (12) and it leads to a set of equations

$$a_1q_1(t_p; A, B) + b_1q_1^3(t_p; A, B) = q_2(t_p; A, B), \qquad p = 1, 2, \ldots \tag{13}$$

in which the modal coordinates q_1 and q_2 at time t_p are known quantities and the initial conditions are $q_1(0) = A$, $q_2(0) = B$, and $\dot{q}_1(0) = \dot{q}_2(0) = 0$. Practically, only four equations ($p = 1$–4) are needed to determine the four unknowns a_1, b_1, A, and B through an iterative scheme. However, the number of equations can be more than the number of unknowns for accurate determination of initial conditions and the least-square method is employed in this case. For system of more than two ($n > 2$) modal coordinates, terms higher than the cubic are to be included. It is also found that choosing three of the time t_p at $t_p = 0$, $T/4 + 2m\pi$, and $T/2 + 2m\pi$ (m is any integer) will yield accurate initial conditions for periodic plate motions. The time history of the plate maximum deflection can be obtained from Eq. (2); thus the frequency–maximum deflection relation is determined. The participation value from the rth linear mode to the total deflection is defined as

$$\frac{\max|q_r|}{\sum_{i=1}^{n}\max|q_i|} \tag{14}$$

Thus, the minimum number of the linear modes for an accurate and converged frequency solution can be determined based on the modal participation values. In addition, the derivation of the general Duffing-type modal equations is straightforward and simple. This procedure is especially convenient for generally laminated anisotropic composite plates of complex shape and boundary conditions; however, it is quite difficult, if not impossible, using the classical continuum Galerkin's approach.

Results and Discussion

Assessment of Single-Mode Elliptic Function Solution

The fundamental frequency ratio $\omega/\omega_L = 2.3501$ at $w_{\max}/r = 5.0$ for a simply supported beam obtained by Woinowsky-Krieger[1] using a single-mode and elliptic function is assessed first. The conventional beam element having six (four bending and two axial) DOF is used. A half-beam is modeled with 10, 15, or 20 elements, and the lowest four symmetrical linear modes are used in the Duffing modal equations. Table 1 shows that a 20-element and 3-mode model will yield a converged result. The percentages of participation from each mode for various values of $w_{\max}/r$ are given in Table 2. The modal participation values demonstrate that a single-mode ($n = 1$) will yield an accurate fundamental frequency because the contribution from higher linear modes to the total deflection is negligible (<0.01% for $w_{\max}/r$ up to 5.0). There is a small difference in frequency ratios between the present finite element and the elliptic integral solutions (e.g., 2.3506 vs 2.3501 at $w_{\max}/r = 5.0$). This is due to the difference between the axial forces of the two

Table 1 Convergence of the fundamental frequency ratio at $w_{max}/r = 5.0$ for a simply supported beam

No. of elements and 3 modes	$(\omega/\omega_L)_1$	No. of modes and 20 elements	$(\omega/\omega_L)_1$
10	2.3537	1	2.3506
15	2.3511	2	2.3506
20	2.3506	3	2.3506
——	——	4	2.3506

Table 2 Fundamental and second frequency ratios and the modal participations for a simply supported beam

	Elliptic integral (Ref. 1)	FEM			
			Modal participation, %		
w_{max}/r	$(\omega/\omega_L)_1$	$(\omega/\omega_L)_1$	q_1	q_3	q_5
0.2	1.0038	1.0038	100.0	0.000	0.000
0.4	1.0150	1.0149	100.0	0.000	0.000
0.6	1.0331	1.0331	100.0	0.000	0.000
0.8	1.0580	1.0581	100.0	0.000	0.000
1.0	1.0892	1.0892	100.0	0.000	0.000
2.0	1.3178	1.3179	100.0	0.002	0.000
3.0	1.6257	1.6258	100.0	0.004	0.000
4.0	1.9760	1.9761	99.99	0.005	0.000
5.0	2.3501	2.3506	99.99	0.009	0.000
w_{max}/r	$(\omega/\omega_L)_2$	$(\omega/\omega_L)_2$	q_2	q_4	q_6
0.2	1.0038	1.0038	100.0	0.000	0.000
0.4	1.0150	1.0149	100.0	0.000	0.000
0.6	1.0331	1.0332	100.0	0.000	0.001
0.8	1.0580	1.0582	100.0	00.00	0.001
1.0	1.0892	1.0893	100.0	0.000	0.002
2.0	1.3178	1.3181	99.99	0.000	0.006
3.0	1.6257	1.6260	99.98	0.000	0.015
4.0	1.9760	1.9768	99.98	0.000	0.021
5.0	2.3501	2.3512	99.96	0.000	0.037

approaches, the finite element method (FEM) gives a nonuniform axial force in each element; however, the average value of the axial force for each element is the same as the one in the classic continuum approach.[1] The lowest (2.0310) and the highest (3.3438) frequency ratios at $w_{max}/r = 5.0$ in Ref. 7 are not accurate.

Frequency ratios for higher modes of the simply supported beam are obtained next. A 40-element with 3-antisymmetric mode for the whole beam model is employed for the frequency ratio of the second nonlinear mode. The modal participations shown in Table 2 indicate that a single-mode approach will yield accurate frequency results for the second mode. And the frequency ratios for the second mode are the same as those of the fundamental one. Thus, the present method agrees extremely well with Woinowsky-Krieger's[1] classic single-mode approach.

The time history of the first two symmetric modal coordinates and the beam central displacement, phase plot, and displacement spectral density (DSD) at the maximum beam deflection $w_{max}/r = 5.0$ for the fundamental frequency (or mode) are shown in Fig. 1. The time scale is nondimensional and T_1 is the period of the fundamental linear resonance. Note that although the central displacement response looks like a simple harmonic motion, it does have a small deviation from pure harmonic motion due to the second small peak in the spectrum. This is in agreement with the classical solution that the ratio of the frequency of the second small peak to that of the first dominant peak is 3.

Now we are ready to assess the single-mode fundamental frequency ratio of a simply supported square plate obtained by Chu and Herrmann.[2] A quarter of the plate is modeled with 6×6, 7×7, 8×8, and 9×9 mesh sizes and 1, 2, 4, or 5 symmetrical modes are used. The C^1 conforming rectangular plate element with 24 (16 bending and 8 membrane) DOF is used. The in-plane boundary conditions are $u = v = 0$ on all four edges. Table 3 shows that the 8×8 (64 elements) mesh size in a quarter-plate and 4-mode model should be used for a converged and accurate frequency solution. Table 4 shows the frequency ratios and modal participation values for the lowest three modes at various

Table 3 Convergence of the fundamental frequency ratios for a simply supported square plate[a]

Mesh sizes and 4 modes	$(\omega/\omega_L)_{11}$ at w_{max}/h 1.0	$(\omega/\omega_L)_{11}$ at w_{max}/h 1.4	No. of modes and 8×8 mesh size	$(\omega/\omega_L)_{11}$ at w_{max}/h 1.0	$(\omega/\omega_L)_{11}$ at w_{max}/h 1.4
6×6	1.4174	1.7423	1	1.4058	1.7028
7×7	1.4163	1.7396	2	1.4169	1.7433
8×8	1.4164	1.7403	4	1.4164	1.7403
9×9	1.4164	1.7400	5	1.4163	1.7401

[a]Poisson's ratio $= 0.3$.

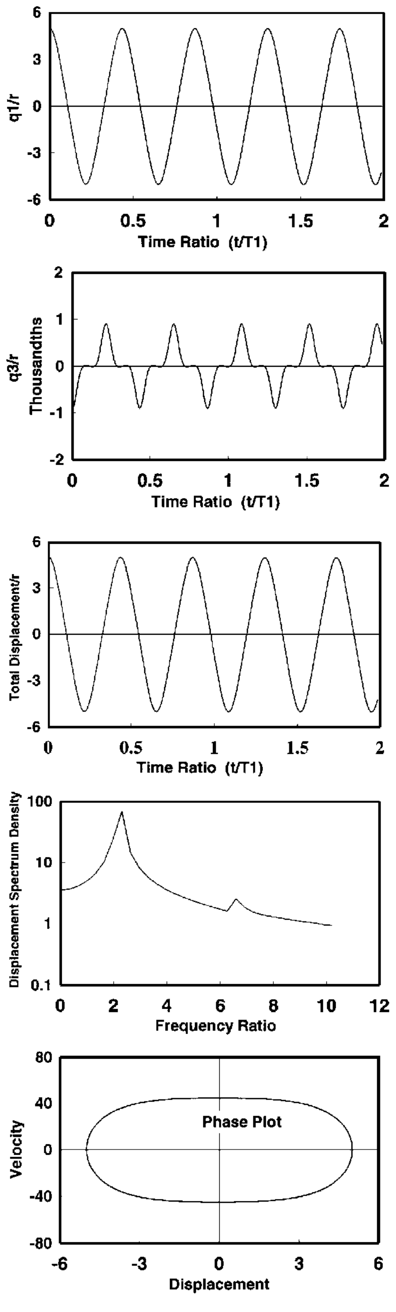

Fig. 1 Time history, phase plot, and DSD for the fundamental mode of a simply supported isotropic beam at $w_{max}/r = 5.0$.

w_{max}/h for a simply supported square plate (8×8 mesh size in a quarter-plate). It indicates that at least two linear modes are needed for an accurate frequency prediction at $w_{max}/h = 1.0$, and the contribution of higher linear modes increase with the increase of plate deflections. The modal participation values also show that the combined modes $(1, 3) - (3, 1)$ and $(2, 4) - (4, 2)$ are independent of the large-amplitude vibrations dominated by (1, 1) and (2, 2) modes, respectively. The time history, phase plot, and

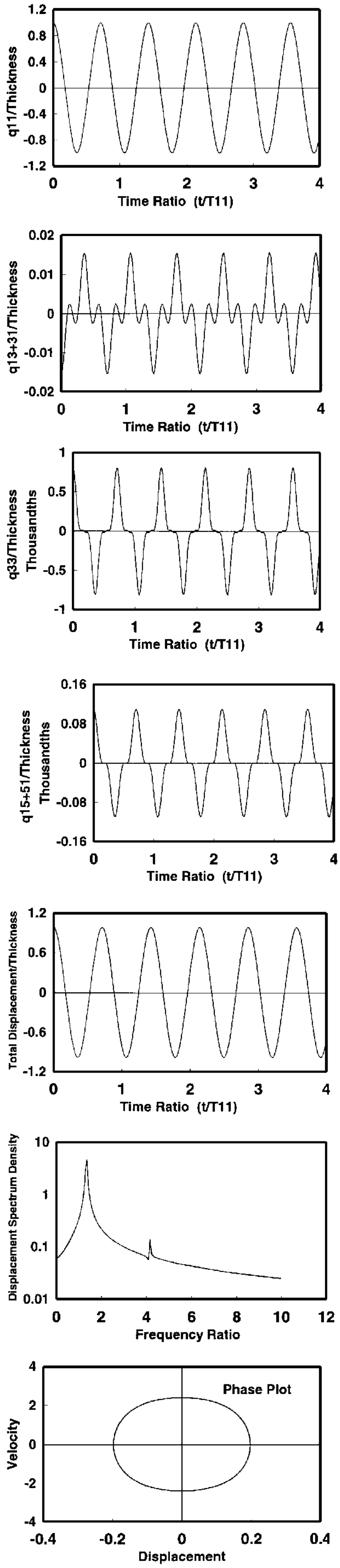

Fig. 2a Time history, phase plot, and DSD for the fundamental mode of a simply supported isotropic square plate at $w_{max}/h = 1.0$.

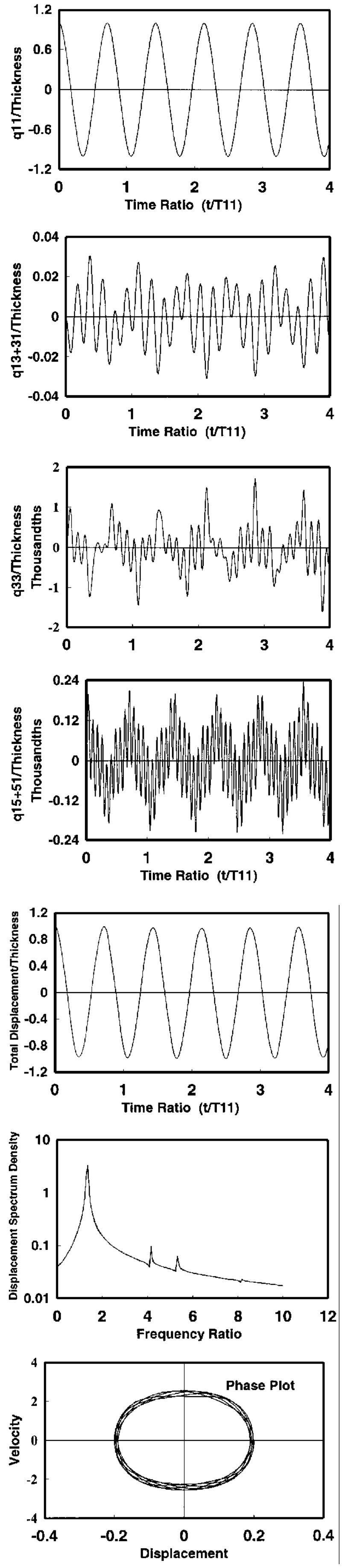

Fig. 2b Nonperiodic modal response using an arbitrary set of initial conditions.

Table 4 Lowest three frequency ratios and the modal participations for a simply supported square plate[a]

w_{max}/h	Elliptic integral (Ref. 2) $(\omega/\omega_L)_{11}$	FEM $(\omega/\omega_L)_{11}$	Modal participation, % q_{11}	$q_{13}+q_{31}$	$q_{13}-q_{31}$	q_{33}	$q_{15}+q_{51}$
0.2	1.0195	1.0195	99.93	0.07	0.00	0.00	0.00
0.4	1.0757	1.0765	99.72	0.27	0.00	0.01	0.00
0.6	1.1625	1.1658	99.38	0.59	0.00	0.02	0.00
0.8	1.2734	1.2796	98.93	1.02	0.00	0.05	0.01
1.0	1.4024	1.4163	98.34	1.57	0.00	0.08	0.01
1.2	1.5448	1.5659	97.54	2.30	0.00	0.15	0.01
1.4	1.6933	1.7401	96.29	3.42	0.00	0.27	0.02
w_{max}/h		$(\omega/\omega_L)_{21}$	q_{21}	q_{23}	q_{41}	q_{43}	
0.2	——	1.0243	99.93	0.06	0.01	0.00	——
0.4	——	1.0976	99.50	0.45	0.03	0.01	——
0.6	——	1.2072	98.15	1.28	0.54	0.02	——
0.8	——	1.3411	97.54	2.41	0.00	0.05	——
1.0	——	1.5126	96.24	3.69	0.00	0.08	——
1.2	——	1.6900	94.90	4.29	0.03	0.15	——
1.4	——	1.8952	93.54	6.01	0.01	0.44	——
w_{max}/h		$(\omega/\omega_L)_{22}$	q_{22}	$q_{24}+q_{42}$	$q_{24}-q_{42}$	q_{44}	
0.2	——	1.0245	100.0	0.00	0.00	0.00	——
0.4	——	1.0751	100.0	0.00	0.00	0.00	——
0.6	——	1.1611	99.99	0.00	0.00	0.01	——
0.8	——	1.2806	99.98	0.01	0.00	0.01	——
1.0	——	1.4041	99.93	0.01	0.00	0.06	——
1.2	——	1.5551	99.97	0.01	0.00	0.01	——
1.4	——	1.7074	99.98	0.02	0.00	0.00	——

[a]Poisson's ratio = 0.3.

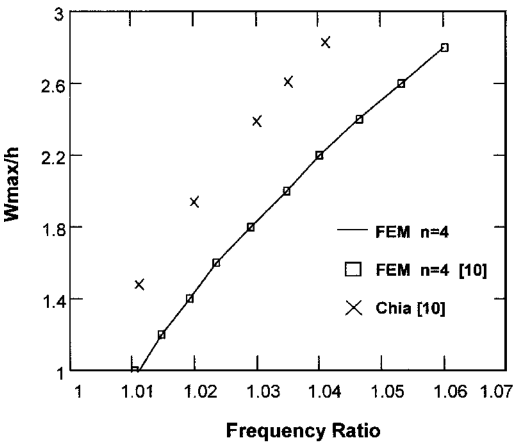

Fig. 3 Amplitude vs fundamental frequency ratio for a clamped orthotropic square plate.

DSD at the maximum deflection $w_{max}/h = 1.0$ for the fundamental mode are shown in Fig. 2a, and T_{11} is the period of the fundamental linear resonance. There is one small peak in the spectrum and the frequency ratio of the second small peak to the first dominant one is 3. The low (1.2967) and the high (1.5314) frequency ratios at $w_{max}/h = 1.0$ given in Ref. 8 are not accurate.

The influence of the initial conditions on periodic motion is demonstrated in Figs. 2a and 2b. In Fig. 2a, the modal coordinates all have the same period, and the initial conditions are determined from Eq. (12). They are $q_{11}(0)/h = 1.0$, $q_{13+31}(0)/h = -0.0155$, $q_{13-31}(0)/h = 0$, $q_{33}(0)/h = 0.000813$, and $q_{15+51}(0)/h = 0.00011$; and initial velocities are null, whereas in Fig. 2b, $q_{11}(0)/h = 1.0$ and all other null are used as the initial conditions. The modal coordinates do not have the same period.

Orthotropic Plate

A clamped square orthotropic composite ($E_1/E_2 = 40$) plate is investigated. A 21×9 finite element mesh is used to model a quarter-plate. The edges of the plate are free from membrane forces; that is, u and v are free at the edges, $u = 0$ along the vertical centerline, and $v = 0$ along the horizontal centerline. The finite element linear vibration analysis from Eq. (3) showed that the modes in increasing frequency are (1, 1), (1, 3), (1, 5), (1, 7), (3, 1), and (3, 3). The finite element fundamental frequency ratios obtained by using the first four modes—(1, 1), (1, 3), (1, 5), and (1, 7)—are shown in Fig. 3. The analytical approximate solutions obtained by Prabhakaran and Chia[10] using modes (1, 1), (1, 3), (3, 1), and (3, 3) are also given in Fig. 3, and it can be seen that the present results agree reasonably well with the four-mode analytical approximate solutions. The four-mode finite element frequency results using Chia's four modes—(1, 1), (1, 3), (3, 1), and (3, 3)—are also given in Fig. 3. The convergence of the nonlinear frequency has clearly indicated that at least two modes are needed. This is demonstrated by the participation values shown in Table 5. The participation value of the second linear mode is more than 7% at $w_{max}/h = 2.8$.

Table 5 Frequency ratios and the modal participations for a clamped orthotropic square plate

w_{max}/h	$(\omega/\omega_L)_{11}$	Modal participation, % q_{11}	q_{13}	q_{15}	q_{17}
0.2	1.0002	99.89	0.11	0.00	0.00
0.4	1.0013	99.58	0.41	0.01	0.00
0.6	1.0044	99.11	0.88	0.01	0.00
0.8	1.0075	98.52	1.47	0.01	0.00
1.0	1.0110	97.87	2.13	0.00	0.00
1.2	1.0147	97.16	2.82	0.02	0.01
1.4	1.0192	96.44	3.51	0.04	0.01
1.6	1.0235	95.73	4.19	0.08	0.00
1.8	1.0291	95.04	4.83	0.13	0.00
2.0	1.0348	94.37	5.44	0.18	0.01
2.2	1.0400	93.73	6.02	0.23	0.02
2.4	1.0463	93.13	6.55	0.29	0.03
2.6	1.0531	92.56	7.05	0.35	0.04
2.8	1.0599	92.02	7.51	0.41	0.06

Figure 4 shows the time history, phase plot, and DSD obtained by using the lowest four modes at $w_{max}/h = 1.0$. It can be seen that the free vibration is simple harmonic and there is one dominant peak only in DSD. This is because $q_{11}(t)$ and $q_{13}(t)$ are both harmonic and have the same period.

Symmetric Composite Plates

A simply supported eight-layer symmetrically laminated $(0/45/-45/90)_s$ composite plate is investigated; the aspect ratio is 2. The graphite/epoxy material properties are as follows:

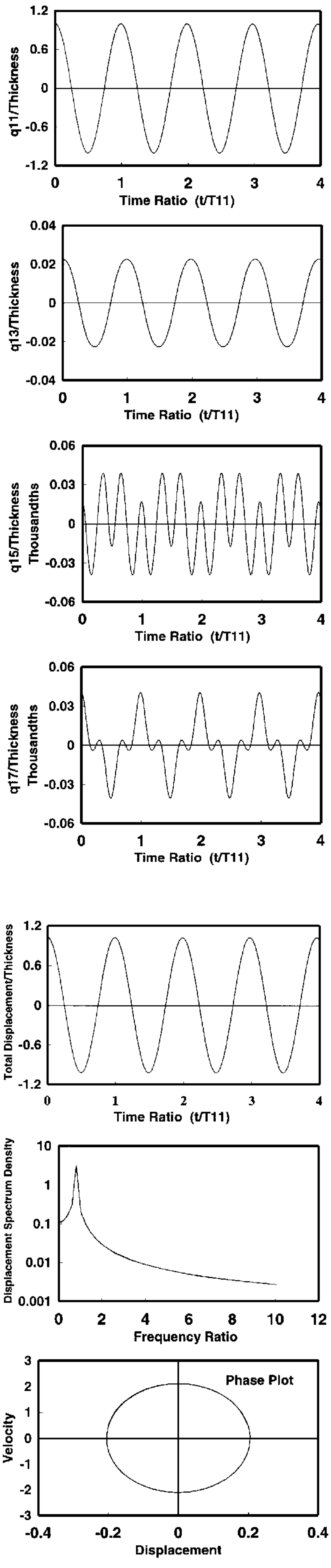

Fig. 4 Time history, phase plot, and DSD for a clamped orthotropic square plate at $w_{max}/h = 1.0$.

Table 6 Frequency ratios and modal participations for a simply supported eight-layer symmetrically laminated $(0/45/-45/90)_s$ composite plate ($a/b = 2$)

		Modal participation, %						
w_{max}/h	$(\omega/\omega_L)_{11}$	q_{11}	q_{12}	q_{21}	q_{13}	q_{22}	q_{23}	q_{31}
0.2	1.0408	99.51	0.00	0.00	0.41	0.07	0.00	0.02
0.4	1.1490	96.57	0.00	0.00	3.01	0.24	0.00	0.17
0.6	1.3484	92.93	0.00	0.00	4.55	0.47	0.00	2.04
0.8	1.5241	98.51	0.00	0.00	0.53	0.94	0.00	0.02
1.0	1.7190	97.43	0.00	0.00	2.39	0.11	0.00	0.07
1.2	1.9258	95.78	0.00	0.00	3.57	0.62	0.00	0.02
1.4	2.1409	94.27	0.00	0.00	4.84	0.77	0.00	0.13

Table 7 Third frequency ratios and the modal participation for a simply supported beam

		Modal participation, %				
w_{max}/r	$(\omega/\omega_L)_3$	q_1	q_3	q_5	q_7	q_9
0.2	1.0037	0.000	100.0	0.000	0.000	0.000
0.4	1.0149	0.000	100.0	0.000	0.000	0.001
0.6	1.0332	0.000	100.0	0.000	0.000	0.002
0.8	1.0582	0.000	100.0	0.000	0.000	0.003
1.0	1.0894	0.000	100.0	0.000	0.000	0.004
2.0	1.3184	0.000	99.99	0.000	0.000	0.014
3.0	1.6268	0.000	99.97	0.000	0.000	0.036
4.0	1.9777	0.000	99.95	0.000	0.000	0.048
5.0	2.3524	0.000	99.92	0.000	0.000	0.082

Young's moduli $E_1 = 22.5 \times 10^6$ psi (155 GPa), $E_2 = 1.17 \times 10^6$ psi (8.07 GPa), shear modulus $G_{12} = 0.66 \times 10^6$ psi (4.55 G Pa), Poisson's ratio $\nu_{12} = 0.22$, and mass density $\rho = 0.1458 \times 10^{-3}$ lb $\cdot$ s^2/in.^{4} (1550 kg/m^3). A 16×8 mesh is used to model the plate. The in-plane boundary conditions are immovable at all four edges. First, seven linear modes are used as the modal coordinates. Table 6 gives the fundamental frequency ratios and mode participation values for the linear modes in increasing frequency order. The modal participation values indicate clearly that only three modes are needed in predicting the nonlinear frequency for w_{max}/h up to 1.4, and three of the seven are independent of the fundamental nonlinear mode. Figure 5 shows the time-history, phase plot, and DSD at $w_{max}/h = 1.0$.

Frequency Ratio for Higher Mode

The second frequency ratio $(\omega/\omega_L)_2$ shown in Table 2 for a simply supported beam and the frequency ratios $(\omega/\omega_L)_{21}$ and $(\omega/\omega_L)_{22}$ in Table 4 for a simply supported square plate are not truly higher frequency ratios in the sense of application of finite element methods. In reality they are the lowest frequency ratios in a proper selection of the boundary conditions to a half-beam or to a quarter-plate model, respectively. To demonstrate that the present FEM will truly predict frequency for higher mode, a half-beam is modeled with 40 elements and the 5 lowest symmetrical modes are included in the Duffing modal equations. The third frequency ratios and participation values are shown in Table 7. The modal participations indicate that a single-mode will yield accurate frequency results.

The higher frequency ratio $(\omega/\omega_L)_{13+31}$ is also obtained for the simply supported square plate shown in Table 8. The quarter-plate is modeled with 8×8 mesh size. The first five linear modes are included in the Duffing equations. The modal participation values reveal a rather interesting nonlinear vibration characteristic that the combined linear mode (1, 3) − (3, 1) is independent of the large-amplitude vibration dominated by (1, 3) + (3, 1) mode.

The higher frequency ratio $(\omega/\omega_L)_{13}$ is also obtained for the simply supported eight-layer symmetrically laminated $(0/45/-45/90)_s$ composite plate. The plate is modeled with a 16×8 mesh size. The modal participation values are given in Table 9, and again only four modes are needed (also see Table 6) for accurate frequency predictions. The time history, phase plot, and DSD at $w_{max}/h = 1.0$ are shown in Fig. 6. The frequency ratio of the second peak to the first one is 3.

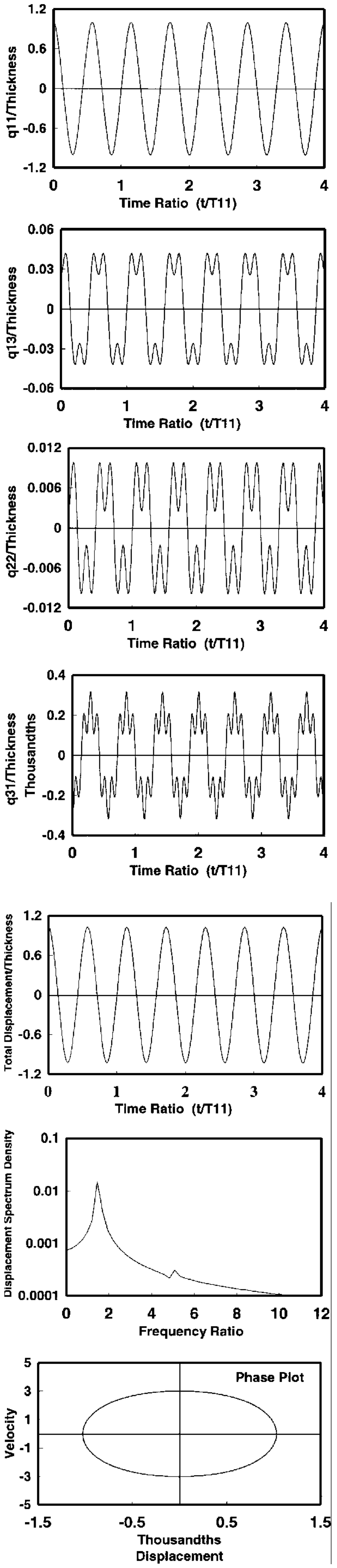

Fig. 5 Time history, phase plot, and DSD for the fundamental mode of a simply supported, eight-layer (0/45/_45/90)$_s$ composite plate at $w_{\max}/h = 1.0$ ($a/b = 2$).

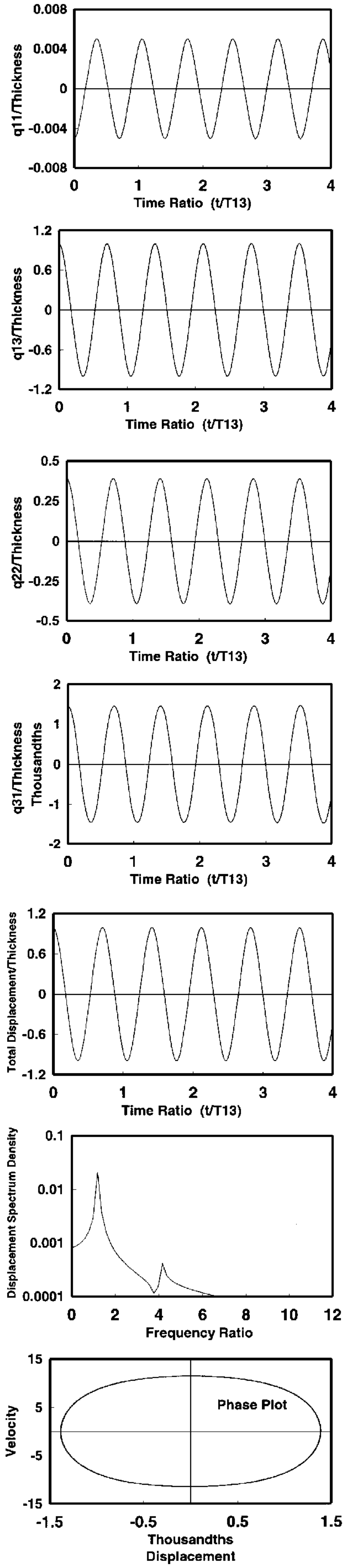

Fig. 6 Time history, phase plot, and DSD for the fourth mode of a simply supported, eight-layer (0/45/_45/90)$_s$ composite plate at $w_{\max}/h = 1.0$ ($a/b = 2$).

Table 8 Third frequency ratios and the modal participations for a simply supported square plate[a]

		Modal participation, %				
w_{max}/h	$(\omega/\omega_L)_{13+31}$	q_{11}	$q_{13}+q_{31}$	$q_{13}-q_{31}$	q_{33}	$q_{15}+q_{51}$
0.2	1.0106	0.14	99.66	0.00	0.17	0.03
0.4	1.0489	0.52	98.68	0.00	0.64	0.16
0.6	1.1086	1.02	97.17	0.00	1.32	0.49
0.8	1.1873	1.52	95.40	0.00	2.10	0.98
1.0	1.2808	1.96	93.58	0.00	2.87	1.59
1.2	1.3923	2.31	91.88	0.00	3.56	2.25
1.4	1.5128	2.58	90.37	0.00	4.13	2.91

[a]Possion's ratio = 0.3.

Table 9 Fourth frequency ratios and modal participations for a simply supported eight-layer symmetrically laminated $(0/45/-45/90)_s$ composite plate ($a/b = 2$)

		Modal participation, %						
w_{max}/h	$(\omega/\omega_L)_{13}$	q_{11}	q_{12}	q_{21}	q_{13}	q_{22}	q_{23}	q_{31}
0.2	1.0214	0.02	0.00	0.00	95.42	4.40	0.00	0.16
0.4	1.0818	0.10	0.00	0.00	86.50	13.08	0.00	0.33
0.6	1.1700	0.22	0.00	0.00	79.07	20.45	0.00	0.26
0.8	1.2891	0.31	0.00	0.00	74.40	25.21	0.00	0.08
1.0	1.4238	0.36	0.00	0.00	71.35	28.00	0.00	0.11
1.2	1.5726	0.37	0.00	0.00	69.70	29.66	0.00	0.26
1.4	1.7340	0.37	0.00	0.00	68.53	30.17	0.00	0.38

Conclusions

A multimode time-domain formulation based on the finite element method is presented for nonlinear free vibrations of composite plates. The use of the FEM enables the present formulation to deal with composite plates of complex geometries and boundary conditions, and the use of the modal coordinate transformation enables us to reduce the number of ordinary nonlinear differential modal equations to a much smaller one. The present procedure is able to obtain the general Duffing-type modal equations easily. Initial conditions for all modal coordinates having the same time period are presented. The participation value of the linear mode is defined quantitatively as the contribution of each linear mode to the nonlinear deflection; they can clearly determine the minimum number of modes needed for accurate nonlinear frequency results.

The present fundamental nonlinear frequency ratios have been compared with the single-mode solution obtained by Woinowsky-Krieger[1] for simply supported beams and by Chu and Herrmann[2] for simply supported square plates and the multimode solution by Prabhakaran and Chia[10] for clamped orthotropic plates, respectively. The Woinowsky-Krieger single-mode solution is accurate. For all other solutions, however, two or more modes are needed. The nonlinear frequency for a simply supported symmetrically laminated rectangular composite plate is also obtained. The phase plot and displacement spectral density showed that nonlinear displacement responses are no longer harmonic. Frequency ratios for higher modes can also be determined using the present FEM. A single-mode solution will give accurate frequency results for simply supported beams. However, multiple modes are required for the isotropic and composite plates.

Acknowledgment

The authors would like to acknowledge the support from the Aerospace Engineering Department, Old Dominion University.

References

[1]Woinowsky-Krieger, S., "The Effect of an Axial Force on the Vibration of Hinged Bars," *Journal of Applied Mechanics*, Vol. 17, No. 1, 1950, pp. 35, 36.

[2]Chu, H. N., and Herrmann, G., "Influence of Large Amplitudes on Free Flexural Vibrations of Rectangular Elastic Plates," *Journal of Applied Mechanics*, Vol. 23, No. 4, 1956, pp. 523–540.

[3]Whitney, J. M., and Leissa, A. W., "Analysis of Heterogeneous Anisotropic Plates," *Journal of Applied Mechanics*, Vol. 36, June 1969, pp. 261–266.

[4]Chia, C. Y., "Geometrically Nonlinear Behavior of Composite Plates: A Review," *Applied Mechanics Review*, Vol. 41, No. 12, 1988, pp. 439–451.

[5]Chia, C. Y., *Nonlinear Analysis of Plates*, McGraw–Hill, New York, 1980.

[6]Sathyamoorthy, M., "Nonlinear Vibrations Analysis of Plates: A Review and Survey of Current Developments," *Applied Mechanics Review*, Vol. 40, No. 11, 1987, pp. 1553–1561.

[7]Srirangaraja, H. R., "Nonlinear Free Vibrations of Uniform Beams," *Journal of Sound and Vibrations*, Vol. 175, No. 3, 1994, pp. 425–427.

[8]Rao, S. R., Sheikh, A. H., and Mukhopadhyay, M., "Large-Amplitude Finite Element Flexural Vibration of Plates/Stiffened Plates," *Journal of the Acoustical Society of America*, Vol. 93, No. 6, 1993, pp. 3250–3257.

[9]Chiang, C. K., Mei, C., and Gray, C. E., Jr., "Finite Element Large-Amplitude Free and Forced Vibrations of Rectangular Thin Composite Plates," *Journal of Vibration and Acoustics*, Vol. 113, July 1991, pp. 309–315.

[10]Prabhakaran, M. K., and Chia, C. Y., "Non-Linear Flexural Vibrations of Orthotropic Rectangular Plates," *Journal of Sound and Vibrations*, Vol. 52, No. 4, 1977, pp. 511–518.